ESTIMATING FOREST SURFACE TEMPERATURE: A CASE STUDY IN CANARY ISLANDS (SPAIN)

A. Barreto, M. Arbelo, P. A. Hernandez-Leal, L. Núñez-Casillas, A. González-Calvo

Grupo de Observación de la Tierra y la Atmósfera. Departamento de Física FEES.
Universidad de La Laguna. 38206 La Laguna. Spain. afriba@ull.es

KEY WORDS: Forestry, Forest fire, Simulation, Comparison, Estimation, Algorithms, Temperature

ABSTRACT:

The forest temperature is one key parameter in the models developed for providing early fire risk alerts. The satellite remote sensing data are the best way to obtain this parameter both regionally and globally. This study proposes an approach to obtain Forest Surface Temperature (FST) by means of Terra-ASTER (Advanced Spaceborne Thermal Emission and Reflectance Radiometer) multiband algorithms. We have proposed a multiband (MB) linear model and a Generalized Additive Model (GAM). The algorithms coefficients are obtained from simulated atmospheric data using the radiative transfer code MODTRAN 4.0 and 524 (381 day-time and 143 night-time) atmospheric soundings launched in Tenerife, Canary Island, Spain. These algorithms have been applied to a fully vegetated forest covered with *Pinus canariensis*. GAM algorithm showed improved residual statistics with respect to the MB both for night and day. Differences between ASTER Surface Kinetic Temperature Product (AST-08) and GAM are in the order of the standard performance of ASTER TES algorithm.

1. INTRODUCTION

Forest surface temperature (FST) is an important parameter for many environmental studies, including the energy budget estimation, land cover assessment as well as the early alert of fires through the use of risk indexes that take into account this parameter among others (Hernández-Leal et al., 2008). Thermal Infrared (TIR) remote sensing data provide a unique opportunity to retrieve surface temperature with a suitable spatial resolution and accuracy. The multispectral imaging capability of remote sensors like ASTER, with a five-channel thermal infrared radiometer, allows obtaining surface temperature with a spatial resolution of 90 m. In fact, it is the highest spatial resolution sensor currently available on a polar-orbiting spacecraft (Jimenez-Muñoz et al., 2010). ASTER project provides to users information about surface temperature (AST-08 product) obtained by means of the Temperature and Emissivity Separation (TES) method, developed by Gillespie et al. (1998). This methodology uses an empirical relationship to predict minimum emissivity, ε_{min}, from the surface spectral contrast, and provides results in global conditions with accuracy within ±1.5 K in temperature and ±0.015 in emissivity. However, as Barreto et al. (2010) suggest, it has proven to underestimate emissivity in the case of low spectral contrast surfaces, like water bodies or vegetated surfaces, as well as it tends to amplify any external error, as those introduced by an inaccurate sensor calibration, atmospheric correction, measurements errors or problems in the algorithm itself.

The main goal of this study is to compare two simpler and easy methodologies to obtain FST from ASTER data to be applied to a coniferous forest in Tenerife Island. These methods consist in a multiband (MB) algorithm, based on the differential-absorption effect using a linear combination of the five TIR ASTER bands and a Generalized Additive Model (GAM) in order to minimize possible biases and dispersion usually introduced in traditional linear models. The application of these algorithms was compared to AST-08 product as reference value to evaluate them.

2. DATA AND METHODOLOGY

2.1 Study area

The study area is situated at Tenerife (Figure 1). It is a densely vegetated area covered by *Pinus canariensis*, an endemic conifer of the Canary Islands (Spain). It is located at a mean altitude of 1400 m above sea level, between about 800 m and 2000 m, predominantly in the northern side of the island. In the southern side the woodland becomes sparser. This belt of dense woodland presents climate features which favor an atmospheric vertical profile characterized by a subsidence thermal inversion with a base at a mean altitude of 1254 m (from 1488 m in wintertime to 962 m in summertime) that confine the oceanic and humid air mass in low atmospheric layers.

We have assumed that the pine forest was relatively homogeneous due to the age structure, treetop density and height of the trees do not vary significantly. Therefore, surface temperature and emissivity distribution are not expected to be influenced by spatial and temporal variability effects.

2.2 ASTER data

The ASTER sensor, onboard NASA's Terra satellite, provides 90 m resolution in its five thermal infrared bands (10-14) between 8 and 12 μm. The radiometric accuracy for these five bands are ±3 K at 200-240 K, ±2 K at 240-270 K and ±1 K at 270-340 K, and a radiometric resolution (NEΔT) of 0.3 K at 300 K (Jimenez-Muñoz et al., 2007).

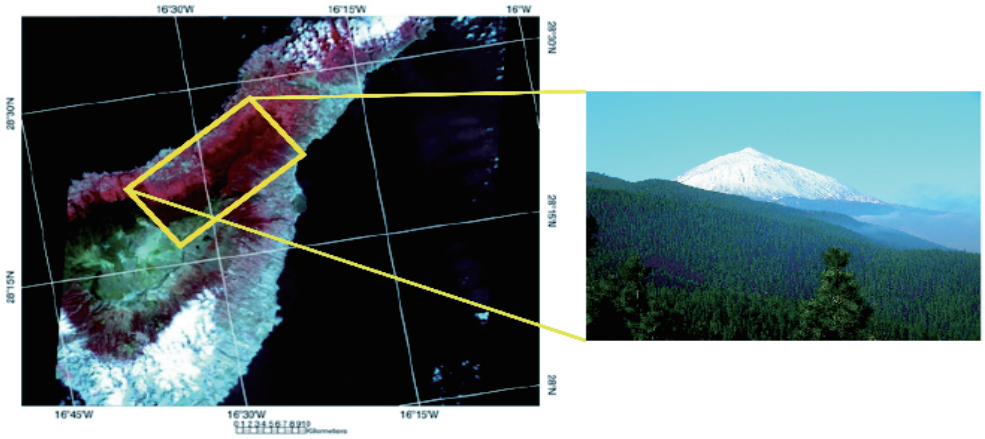

Figure 1. ASTER colour composite of Tenerife Island for April 16, 2008. RGB components are ASTER bands 3 (0.81 µm), 2 (0.66 µm) and 1 (0.56 µm). Zoom image corresponds to a panoramic view of the coniferous forest in the northern side of Tenerife.

2.3 Atmospheric correction and simulation process

Any methodology that attempts to retrieve surface temperature from TIR data must correct for the intervening atmosphere. This correction is based on the radiative transfer equation which is given by the following equation:

$$L_{sensor,j} = \left[\varepsilon_j \cdot B_j(T_s) + (1-\varepsilon_j)\cdot L_j^{\downarrow}\right]\cdot \tau_j + L_j^{\uparrow} \qquad (1)$$

where $L_{sensor,j}$ represents the at-sensor radiance measured by ASTER in a certain channel j, τ_j represents the spectral atmospheric transmittance, $L_j^{\uparrow}$ is the spectral upwelling radiance and $L_j^{\downarrow}$ is the spectral atmospheric downwelling radiance. B_j is the blackbody radiance of a surface at temperature T_s, which coincides with *FST*, and ε_j is the spectral surface emissivity. Atmospheric parameters (τ_j, $L_j{}^{\uparrow}$, $L_j{}^{\downarrow}$ and $L_{sensor,j}$) were retrieved by means of the MODTRAN radiative code (Berk et al., 1999). Due to the important spatial and temporal variability of atmospheric constituents the use of local vertical profiles are considered the ideal method to better characterize the atmosphere and thus develop a more reliable atmospheric correction. 524 cloud-free local atmospheric profiles obtained from January 2006 to December 2008 (381 day and 143 night) were introduced in the radiative code, as well as, six different values for T_s(K), ranging from T_0-5, T_0, T_0+5, T_0+10, T_0+15, and T_0+20 for day data, and T_0-10, T_0-5, T_0, T_0+5, T_0+10 and T_0+15 for night data. T_0 represents the temperature at the first layer in the atmospheric soundings.

In order to account for the complex topography of the island and to avoid the presence of inaccuracies introduced in the atmospheric parameters retrieved over high elevated forest areas, each atmospheric profile was divided into 3 layers, starting from the level of 500 m, 1000 m and 1500 m. Thus, for each profile, there were 3 simulations, one for each base level.

Emissivity of *Pinus canariensis* is also a necessary value to introduce in Equation 1. Emissivity is one of the most important sources of error on this type of methodology. We have considered 17 emissivity spectra for pine forest. Two spectra have been measured by means of the box method in the version of two lids. A thorough description of the mentioned procedure is given by Rubio et al. (2003). We used CIMEL 312-2 infrared radiometer with five (11-11.7 µm, 10.3-11 µm, 8.9-9.3 µm, 8.5-8.9 µm and 8.1-8.5 µm) spectral bands coincident with ASTER bands. Two representative samples of individual trees were extracted, and needle piles were measured simulating the coniferous canopy. The spectral emissivity obtained from the first sample is 0.972±0.004, 0.972±0.009, 0.972±0.008, 0.975±0.005 and 0.971±0.009 for ASTER bands 10 to 14. For the second sample, we obtained a value of 0.958±0.007, 0.960±0.009, 0.958±0.010, 0.930±0.010 and 0.966±0.010, respectively. In addition, in order to assure the representativeness of the spectra used, we have extended emissivity information using the ASTER standard products of surface emissivity (AST-05). We have extracted 15 average emissivity values from fifteen 8x8 pixels test sites uniformly located inside the woodland in terms of spatial location and altitude. It has been done for eight different dates (02/03/2003, 15/09/2005, 26/03/2006, 31/03/2008, 16/04/2008, 02/05/2008, 05/07/2008 and 09/10/2008). The average results are shown in Figure 2.

Taking into account all previous variables, including the 17 emissivities, the 6 first level temperatures and the 3 heights, a total of 116586 day data (381 x 17 x 6 x 3) and 43758 night data (143 x 17 x 6 x 3) were available to develop and validate the algorithms.

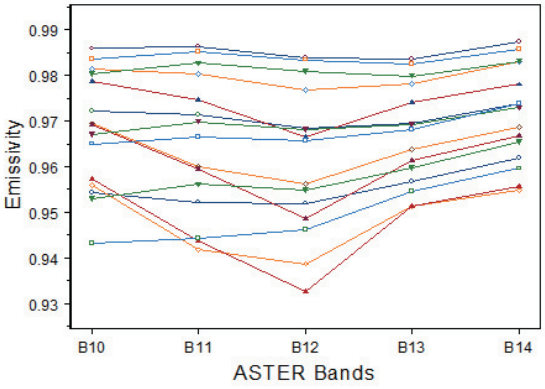

Figure 2. Emissivity spectra extracted from AST-05 products for fifteen test sites and eight different dates in the coniferous forest.

2.4 Multiband algorithm (MB)

MB algorithm has been estimated by regressing the simulated at-sensor brightness temperature from the five ASTER TIR bands (T_i) against the surfaces temperature (T_s) assumed as the first layer temperature from the atmospheric soundings. The functional form of the MB algorithm is:

$$FST_{MB} = a_0 + \sum_{i=1}^{5} a_i \cdot T_i \qquad (2)$$

2.5 GAM algorithm

Generalized Additive Models (GAMs) are an extension of traditional generalized linear models. This nonparametric modelling technique objectively estimates the functional relationship for each predictor term in an additive model such as a *FST* algorithm (Hastie and Tibshirani, 1990). The general form of this formulation is:

$$FST_{GAM} = \alpha + \sum_{i=1}^{q} g_i(X_i) \qquad (3)$$

Where α is a constant term analogous to that in linear regressions (a_0), X_i are the predictor variables and g_i a set of non-linear functions of them. See Arbelo et al. (2005) for further details of GAM methodology applied to satellite sea surface temperature algorithms.

Thus, the main idea of this methodology consists of replacing the usual linear function of a covariate with an unspecified smooth function. In this study we have used cubic smoothing splines (s). The best-fitting was selected by means of an automated backward and forward stepwise selection technique. GAM let us to incorporate height (h) and month (m) as continuous predictor variables, something difficult to introduce in linear algorithms.

3. RESULTS AND DISCUSSION

We developed the fitting procedures for MB and GAM algorithms, both for day and night, using a training set with 2007 and 2008 data, and then computing the T_s (i.e. *FST*) and residuals for a validation set independent from the previous set with 2006 data.

For simplicity, we only show the algorithms for the case of day:

$$FST_{MB} = 0.773T10 - 1.346T11 + 3.886T12 - 2.884T13 + 0.388T14 + 65.17197 \qquad (4)$$

$$FST_{GAM} = 0.544s(T10) - 1.248T11 + 3.824s(T12) - 2.706T13 + 0.419s(T14) + 0.117s(h) + 0.002s(m) \qquad (5)$$

Surprisingly, the GAM model selected as the best included all terms smoothed with degree 10 ($s(Ti)$), except the brightness temperatures of the bands 11 and 13, that were selected as contributing linearly to the model.

To study this circumstance more in depth, the residuals of both algorithms are plotted as a function of the different predictors. We would expect a random dispersion of the residuals around zero line in case of the linear approximation were valid. However, the trend curves presented in the Figures 3 and 4 for the height and the month confirm the presence of an anomalous behaviour in FST_{MB} residuals, suggesting that the linear approximation is not fully appropriate.

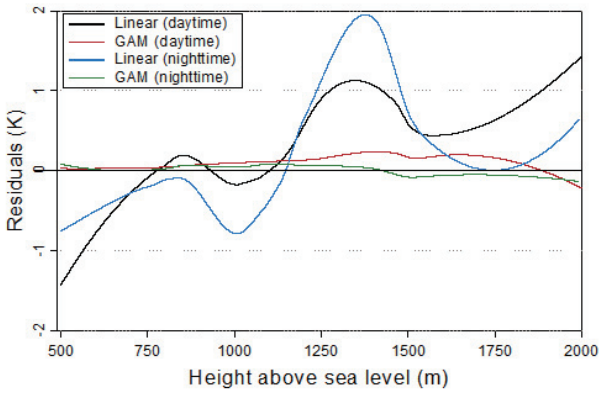

Figure 3. Day and night trend lines fitted to *FST* residuals against height of the first layer considered in the simulation process obtained by means of the linear (MB) and the GAM algorithms.

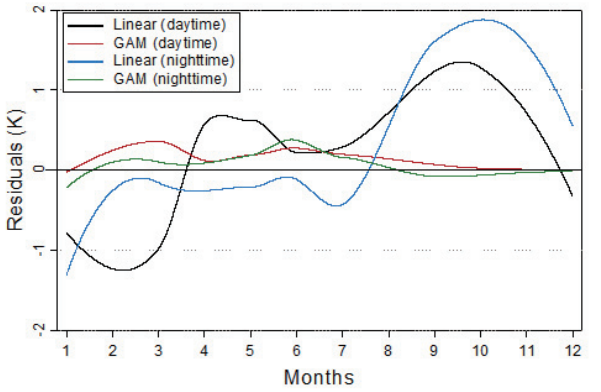

Figure 4. Day and night trend lines fitted to *FST* residuals against the months obtained by means of the linear (MB) and the GAM algorithms.

The global results extracted for MB and GAM algorithms using the independent validation set are summarized in Table 1. The best results are obtained with GAM algorithm, showing a decrease in RMSE, with regard to MB algorithm, of 0.29 K for daytime and 0.44 K for nighttime respectively. Moreover, the same behaviour between day and night are observed in both algorithms, with lower bias and RMSD for nighttime data.

	DAY			NIGHT		
Algorithm	*RMSE*	*BIAS*	*R*	*RMSE*	*BIAS*	*R*
MB	2.89	0.63	0.90	2.87	0.19	0.90
GAM	2.60	0.53	---	2.43	0.09	---

Table 1. RMSE (K), bias (K) and correlation obtained for MB and GAM algorithms for day and night data.

With regard to the emissivity (results not shown), GAM algorithm display an insensitive behaviour, with no significant differences between results obtained for the seventeen spectra used. Meanwhile the linear algorithm, depends slightly on the lower emissivities used in the simulation.

We have also compared the results for *FST* obtained by means of MB and GAM formulation with surface temperature reference values obtained for the 02/02/2003 ASTER AST-08 standard product. To do this, we have selected six test site

uniformly located within the coniferous forest at altitudes ranging from 1711 m to 947 m (Table 2).

ZONE	1	2	3	4	5	6
Height (m)	1415	1701	1711	1585	1094	947
ΔT GAM (K)	-2.48	0.29	-2.36	-2.07	-0.70	0.07
ΔT MB (K)	-2.89	0.44	-2.00	-2.95	-2.56	-1.46

Table 2. Differences (ΔT) between AST-08 temperature product and GAM and MB, for six different sites uniformly located within the coniferous forest for 02/03/2003 (daytime).

For GAM algorithm, a mean error of -1.21 K was observed including all zones, as well as a RMSE of 1.74 K. The differences found are in the order of the standard performance of ASTER TES (Gillespie et al., 1998). However, the linear algorithm results are above these values by almost 1 K.

4. CONCLUSIONS

We have proposed two alternative algorithms to the TES, which has traditionally been used with ASTER data for deriving the surface temperature. Both algorithms are independent of local atmospheric conditions at the time of image capture, as well as the emissivity of the surface, because we considered their application only to homogeneous Canary pine forests that crown the island of Tenerife. GAM algorithm showed improved residual statistics with respect to the MB. The behaviour of FST_{GAM} residuals was fairly uniform for a broad range of heights, time of year and emissivities.

5. ACKNOWLEDGEMENTS

This work was supported by the Projects CGL2007-66888-C02-01/CLI and PCT-MAC 2007-2013 (FEDER).

6. REFERENCES

Arbelo, M., Podestá, G., Evans, R. and Katherine Kilpatrick, 2005. Improving global satellite-based sea surface temperature climatologies. Recent research developments in thermal remote sensing, Research Signpost, Kerala, India, pp.67-88.

Barreto, A., Arbelo, M., Hernández-Leal, P. A., Núñez-Casillas, L., Mira, M. and C. Coll, 2010. Evaluation of surface temperature and emissivity derived from ASTER data: a case study using ground-based measurements at a volcanic site. *J. Atmos. Ocean Tech.*, in press.

Berk, A., G. P. Anderson, P. K. Acharya, J. H. Chetwyn, L. S. Berstein, E. P. Shettle, et al., 1999. Modtran 4 user's manual. Air Force Research Laboratory, Space Vehicles Directorate, Air Force Materiel Command, Hascom AFB, MA, 95 pp.

Gillespie, A. R., T. Matsunaga, S. Rokugawa, and S. J. Hook, 1998. Temperature and emissivity separation from Advanced Spaceborne Thermal Emission and Reflection Radiometer (ASTER) images. *IEEE Trans. Geosci. Remote Sens.*, **36**, 4, pp. 1113-1125.

Hastie, T. J., and R. J. Tibshirani, 1990: Generalized Additive Models, Chapman and Hall, London, 335 pp.

Hernandez-Leal, P. A., González-Calvo, A., Arbelo, M.; Barreto, A. and A. Alonso-Benito, 2008. Synergy of GIS and Remote Sensing Data in Forest Fire Danger Modeling. IEEE *Journal of Selected Topics in Applied Earth Observations and Remote Sensing*. **1**(2), pp. 240-247.

Rubio, E., V. Caselles, C. Coll, E.Valor and F. Sospedra, 2003. Thermal-infrared emissivities of natural surfaces: improvements on the experimental set-up and new measurements. *Int. J. Remote Sens.*, **24**, 24, pp. 5379-5390.

Jiménez-Muñoz, J. C. and J. A. Sobrino, 2007. Feasibility of retrieving land surface temperature from ASTER TIR bands using two-channel algorithms: a case study of agricultural areas. *IEEE Geoscience and Remote Sensing Letters,* **4** (1), pp. 60-64.

Jimenez-Munoz, J. C. and J. A. Sobrino, 2010. A Single-Channel Algorithm for Land-Surface Temperature Retrieval From ASTER Data. *IEEE Geoscience and Remote Sensing Letters*, **7**, issue 1, pp. 176-179.